J|A|C|S ARTICLES

Published on Web 10/14/2010

Amphiphilic Polyethylenes Leading to Surfactant-Free Thermoresponsive Nanoparticles

Vladimir A. Kryuchkov,[†] Jean-Christophe Daigle,[‡] Kirill M. Skupov,[†,‡] Jérome P. Claverie,*[,‡] and Françoise M. Winnik*[,†]

Département de Chimie, Pavillon J.A. Bombardier, Université de Montréal, CP 6128, Succursale Centre Ville, Montréal, QC, H3C 3J7, Canada, and NanoQAM, Functional Materials Research Center, Département de Chimie, Université du Québec á Montréal, Succursale Centre Ville, Montréal, QC, H3C 3P8, Canada

Received May 14, 2010; E-mail: francoise.winnik@umontreal.ca

Abstract: Linear copolymers of ethylene and acrylic acid (PEAA) were prepared by catalytic polymerization of ethylene and *tert*-butyl acrylate followed by hydrolysis of the ester groups. The copolymers contained COOH groups inserted into the crystalline unit cell with formation of intramolecular hydrogen-bonds, as established on the basis of differential scanning calorimetry (DSC), Fourier-transform infrared spectroscopy (FTIR), and X-ray diffraction (XRD) studies. A solvent-exchange protocol, with no added surfactant, converted a solution in tetrahydrofuran of a PEAA sample containing 12 mol % of acrylic acid (AA) into a colloidally stable aqueous suspension of nanoparticles. Transmission electron microscopy (TEM), dynamic light scattering (DLS), and high sensitivity differential scanning calorimetry (HS-DSC) were used to characterize the nanoparticles. They are single crystals of elongated shape with a polar radius of 49 nm ($\sigma = 15$ nm) and an equatorial radius of 9 nm ($\sigma = 3$ nm) stabilized in aqueous media via carboxylate groups located preferentially on the particle/water interface. The PEAA (AA: 12 mol %) nanoparticles dispersed in aqueous media exhibited a remarkable reversible thermoresponsive behavior upon heating/cooling from 25 to 80 °C.

Introduction

Polymeric nanoparticles are the focus of intensive research in view of their numerous applications in areas such as nanomedicine,[1−4] imaging,[5,6] diagnostics,[7] chemical separations,[8,9] sensors,[8] catalysis,[10,11] and colloidal crystals.[12] They are obtained by self-assembly of copolymers consisting of hydrophobic and hydrophilic fragments, or amphiphilic copolymers. There exist currently a plethora of such polymers with various degrees of structural complexity, which are synthesized by all types of polymerizations and also obtained by modification of natural polymers. Yet, only a few nanoparticles based on amphiphilic copolymers of ethylene have been reported to date. Copolymers of ethylene and hydrophilic charged monomers are well-known as typical examples of ionomers, which are thermoplastic polymers that contain a small fraction of pendant ionic functional groups.[13] For instance, random copolymers of ethylene and methacrylic acid, approximately 85:15 mol:mol, where some of the acid groups are converted to metal salts, are commercially important polymers extensively used in a variety of applications, including orthodics and prosthetics, as films, adhesive layers in foil/paper containers, and as constituents of items such as golf balls and bowling pins. In bulk, they contain amorphous and crystalline polyethylene phases as well as ionic clusters acting as physical cross-links.[13,14] The introduction of the ionic groups greatly improves the mechanical and optical properties of the copolymers. A limited number of studies of ionomers in water were carried out in the late 1990s, especially by the group of Schlick, who probed the microstructure of polymeric micelles formed in aqueous solutions of poly[ethylene-co-(potassium methacrylate)] with 7.5 mol % methacrylate (M_n

[†] Universite de Montréal.
[‡] Université du Québec á Montréal.

(1) Pan, D.; Williams, T. A.; Senpan, A.; Allen, J. S.; Scott, M. J.; Gaffney, P. J.; Wickline, S. A.; Lanza, G. M. *J. Am. Chem. Soc.* **2009**, *131*, 15522–15527.
(2) Chu, L. Y.; Kim, J. W.; Shah, R. K.; Weitz, D. A. *Adv. Funct. Mater.* **2007**, *17*, 2291–2297.
(3) Savic, R.; Luo, L.; Eisenberg, A.; Maysinger, D. *Science* **2003**, *300*, 615–618.
(4) Dhar, S.; Gu, F. X.; Langer, R.; Farokhzad, O. C.; Lippard, S. J. *Proc. Natl. Acad. Sci. U.S.A.* **2008**, *105*, 17356–17361.
(5) Kim, K.; Lee, M.; Park, H.; Kim, J.-H.; Kim, S.; Chung, H.; Choi, K.; Kim, I. S.; Seong, B. L.; Kwon, I. C. *J. Am. Chem. Soc.* **2006**, *128*, 3490–3491.
(6) Zhou, M.; Xing, F.; Ren, M.; Feng, Y.; Zhao, Y.; Qiu, H.; Wang, X.; Gao, C.; Sun, F.; He, Y.; Ma, Z.; Wen, P.; Gao, J. *ChemPhysChem* **2009**, *10*, 523–526.
(7) Akbulut, M.; Ginart, P.; Gindy, M. E.; Theriault, C.; Chin, K. H.; Soboyejo, W.; Prud'homme, R. K. *Adv. Funct. Mater.* **2009**, *19*, 718–725.
(8) Satish, N.; Lyon, L. A. *Angew. Chem.* **2005**, *44*, 7686–7708.
(9) Kawaguchi, H.; Fujimoto, K. *Bioseparation* **1998**, *7*, 253–258.
(10) Bergbreiter, D. E.; Case, B. L.; Liu, Y. S.; Waraway, J. W. *Macromolecules* **1998**, *31*, 6053–6062.
(11) Bergbreiter, D. E.; Tian, J.; Hongfa, C. *Chem. Rev.* **2009**, *109*, 530–582.
(12) Debord, J. D.; Eustis, S.; Debord, S. B.; Lofye, M. T.; Lyon, L. A. *Adv. Mater.* **2002**, *14*, 658–662.
(13) Tant, M. R.; Wilkes, G. L. In *Ionomers: synthesis, structure, properties and applications*; Tant, M. R., Wilkes, G. L., Eds.; Chapman & Hall: London, 1997; p 261−289.
(14) Eisenberg, A. *Macromolecules* **1970**, *3*, 147–154.

= 20 500 g/mol, PDI = 4).[15,16] Using fluorescence and electron spin resonance spectroscopy, they determined that the particles have an amorphous core formed by the hydrophobic PE fragments surrounded by an external shell in which the polar groups are concentrated. A new class of amphiphilic polyolefins prepared by metathesis,[17−19] the so-called precision polyolefins, where the polar substituents are always separated by the same number of methylene groups, are expected to show interesting properties in aqueous media, but the study of their self-assembly is still in its infancy.[20] Emrick et al. have reported recently a preparation, by ring-opening metathesis polymerization, of amphiphilic polyolefins bearing a wide range of polar groups.[21−23] Phosphorylcholine-substituted polyolefins were shown to self-assemble in water into stable "polymersomes", which are promising biomimetic materials.[23] Polymers of this type are amorphous and soluble in organic solvents at room temperature. Hence, they differ greatly from conventional polyolefins, which are crystalline and insoluble in any organic solvent at room temperature.

From a mechanistic viewpoint, the self-assembly in water of crystalline polyethylene bearing polar groups presents fascinating aspects, since it is expected to be directed not only by the balance between hydrophilic and hydrophobic interaction energies, but also by the propensity of PE to crystallize, in contrast to the situation with amorphous amphiphilic polymers. The crystallization driving force may, in fact, be critical, if one judges from recent reports from the group of Mecking on the formation of pure polyethylene nanoparticles (∼10 nm) upon catalytic polymerization of ethylene in water using water-soluble catalysts and surfactants.[24] The core of the nanoparticles consists of single lamella hexagonal PE crystals of narrow size distribution and thickness (6.3 nm). The nanoparticles owe their stability in water to the presence of a surfactant shell acting as colloidal stabilizer.[25] A study by Li et al. of the self-assembly in water of linear polyethylene-*b*-poly(ethylene oxide) also points to the importance of the tendency of PE toward crystallization.[26] In water at room temperature polyethylene-*b*-poly(ethylene oxide) copolymers form multicore micelles believed to result from the aggregation of smaller single core polymeric micelles with a crystalline central PE phase.

Crystalline polyethylene is readily prepared by catalytic polymerization of ethylene. However, the insertion of polar comonomers along the polyethylene backbone by catalytic polymerization constitutes a considerable synthetic challenge, since polar functional groups interfere with the catalytic process via various deactivation processes.[27] Nonetheless, over the last decades important progress has been made toward achieving the catalytic synthesis of linear ethylene copolymers containing polar functionalities.[27] Several synthetic routes have been reported, yielding polymers bearing pendant ester,[28−30] nitrile,[31] amide,[32] *N*-carboxyl,[32] and ether groups.[33] We report here the first preparation by catalytic polymerization of linear crystalline ethylene and *tert*-butyl acrylate (TBA) random copolymers with various degrees of acrylate incorporation. These copolymers are readily converted to the corresponding poly(ethylene-co-acrylic acid)s (PEAA) (Scheme 1), which are excellent candidates for testing the impact of the driving force toward crystallization on the self-assembly of amphiphilic polymers. We used a room temperature, surfactant-free solvent-exchange method to trigger the self-assembly of PEAA samples in neutral (pH 7) water. This process yielded crystalline nanoparticles of remarkable colloidal stability in water over a wide range of temperatures and pHs. We also describe how the level of AA incorporation along the PE chains directs the copolymer self-assembly in water, and we examine the influence of crystallinity on the process. Finally, we demonstrate, using high-sensitivity microcalorimetry and dynamic light scattering, that colloidal aqueous PEAA nanoparticles exhibit a reversible thermosensitivity driven by the fusion/crystallization of their polyethylene core. To our knowledge, this is the first time that thermosensitivity is observed for a colloidal polyolefin.

Scheme 1. Preparation of the Polymers

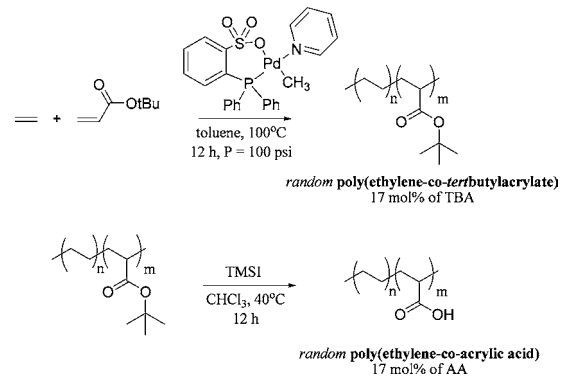

Results and Discussion

Preparation and Characterization of Poly(ethylene-co-acrylic acid) Samples. The copolymers were prepared by catalytic copolymerization of C_2H_4 with TBA and deprotection of the *tert*-butyl ester to afford PEAA (Scheme 1). The copolymerization of TBA with C_2H_4 was conducted using catalyst

(15) Kutsumizu, S.; Schlick, S. *J. Mol. Struct.* **2005**, *739*, 191–198.
(16) Szajdzinska-Pietek, E.; Wolszczak, M.; Plonka, A.; Schlick, S. *J. Am. Chem. Soc.* **1998**, *120*, 4215–4221.
(17) Baughman, T. W.; Chan, C. D.; Winey, K. I.; Wagener, K. B. *Macromolecules* **2007**, *40*, 6564–6571.
(18) Opper, K. L.; Wagener, K. B. *Macromol. Rapid Commun.* **2009**, *30*, 915–919.
(19) Opper, K. L.; Fassbender, B.; Brunklaus, G.; Spiess, H. W.; Wagener, K. B. *Macromolecules* **2009**, *42*, 4407–4409.
(20) Berda, E. B.; Lande, R. E.; Wagener, K. B. *Macromolecules* **2007**, *40*, 8547–8552.
(21) Breitenkamp, K.; Simeone, J.; Jin, E.; Emrick, T. *Macromolecules* **2002**, *35*, 9249–9252.
(22) Breitenkamp, R. B.; Ou, Z.; Breitenkamp, K.; Muthukumar, M.; Emrick, T. *Macromolecules* **2007**, *40*, 7617–7624.
(23) Kratz, K.; Breitenkamp, K.; Hule, R.; Pochan, D.; Emrick, T. *Macromolecules* **2009**, *42*, 3227–3229.
(24) Tong, Q.; Krumova, M.; Gottker-Schnetmann, I.; Mecking, S. *Langmuir* **2008**, *24*, 2341–2347.
(25) Weber, C. H. M.; Chiche, A.; Krausch, G.; Rosenfeldt, S.; Ballauff, M.; Harnau, L.; Göttker-Schnetmann, I.; Tong, Q.; Mecking, S. *Nano Lett.* **2007**, *7*, 2024–2029.
(26) Li, T.; Wang, W. J.; Liu, R.; Liang, W. H.; Zhao, G. F.; Li, Z. Y.; Wu, Q.; Zhu, F. M. *Macromolecules* **2009**, *42*, 3804–3810.
(27) Nakamura, A.; Ito, S.; Nozaki, K. *Chem. Rev.* **2009**, *109*, 5215–5244.
(28) Drent, E.; van Dijk, R.; van Ginkel, R.; van Oort, B.; Pugh, R. I. *Chem. Commun.* **2002**, 744–745.
(29) Skupov, K. M.; Marella, P. R.; Simard, M.; Yap, G. P. A.; Allen, N.; Conner, D.; Goodall, B. L.; Claverie, J. P. *Macromol. Rapid Commun.* **2007**, *28*, 2033–2038.
(30) Skupov, K. M.; Hobbs, J.; Marella, P. R.; Golisz, S.; Goodall, B. L.; Claverie, J. P. *Macromolecules* **2009**, *42*, 6953–6963.
(31) Kochi, T.; Noda, S.; Yoshimura, K.; Nozaki, K. *J. Am. Chem. Soc.* **2007**, *129*, 8948–8949.
(32) Skupov, K. M.; Piche, L.; Claverie, J. P. *Macromolecules* **2008**, *41*, 2309–2310.
(33) Luo, S.; Vela, J.; Lief, G. R.; Jordan, R. F. *J. Am. Chem. Soc.* **2007**, *129*, 8946–8947.

Table 1. Physical Properties of the Polymers

monomer incorporation x,[a] mol %	PETBAx				PEAAx		
	M_n,[b] g/mol	PDI[b]	T_m (°C)[c]	$\Delta H_{melting}$(J/g)[c]	T_m (°C)[c]	$\Delta H_{melting}$(J/g)[c]	COOH[d] mol %
4	7800	1.5	102	103	nd	nd	nd
7	5800	1.9	90	59	114	99	nd
10	3800	1.3	66	32	80	79	nd
12	3000	1.2	60	18	76	44	12.0
16	3000	1.2	42	9	62	12	15.9
17	2800	1.2	nd[e]	nd	nd	nd	17.1

[a] Determined by ^{1}H NMR analysis. [b] Determined by GPC analysis at 160 °C in 1,2,4 trichlorobenzene. [c] Determined by DSC of the solid sample. [d] Determined by conductometric titration. [e] Not determined.

1 (Scheme 1) developed previously for the copolymerization of ethylene with methyl acrylate.[28−30,34,35] The level of TBA incorporation was determined by ^{1}H NMR spectroscopy, by comparing the integral of the methine proton resonance CH(COO-^{t}Bu) to that of all other resonances (Figures S1−S3, Supporting Information). The absence of acrylate dyads in the quantitative ^{13}C NMR spectra of the copolymers (Figure S3, Supporting Information) was taken as evidence that each acrylate unit is separated from another one by one ethylene unit or more. By varying the monomer feed in the copolymerization (i.e., acrylate concentration or ethylene pressure), we obtained six linear copolymers of ethylene and TBA (PETBA) containing from 4 to 17 mol % acrylate (Table 1). For the sake of brevity, the notation PETBAx (respectively PEAAx) will designate the copolymer incorporating x mol % of TBA (respectively AA).

For the second step, we set out to hydrolyze the TBA groups with anhydrous trifluoroacetic acid, a method frequently used to carry out polymer-analogous conversion of the *tert*-butyl ester group into a carboxylic acid.[36] For solubility reasons, the reaction was carried out in an anhydrous mixture of dichlorobenzene and trifluoroacetic acid (80:20 v:v) at 90 °C. The reaction progress was monitored by following the disappearance of the ester carbonyl stretching band at 1730 cm^{-1} in the FTIR spectrum of the mixture. The appearance of two bands, one at 1706 cm^{-1}, attributed to the stretching vibration of isolated carbonyls of COOH groups, the other one at 1743 cm^{-1}, attributed to H-bonded COOH dimers,[37] confirmed the success of the conversion (see Figure S7, Supporting Information). Unfortunately, the polymers recovered *in their dry form* after purification resisted dissolution in any solvent. Their insolubility is attributed to the formation, in the absence of water, of an extensive H-bond network among carboxylic acid groups, as evidenced by the FTIR spectrum of the samples. These polymers were not used for further manipulations. To circumvent this insolubility problem, we used a different method known to cleave esters into carboxylic acids under milder conditions.[38−40] The ester groups of PETBAx were converted into trimethylsilyl carboxylates by treatment with trimethylsilyl iodide. Subsequent aqueous hydrolysis led to PEAAx which were not involved in extensive H-bond networks, as shown by the samples FTIR spectra, which presented a band in the carbonyl stretching spectral region located at 1704 cm^{-1}, a wavenumber typical of the stretching of carbonyls of isolated COOH, together with a broad absorption in the 3000 cm^{-1} region due to the presence of H-bonds with traces of water (from the final hydrolysis step). The FTIR spectra presented only a minute absorption at 1743 cm^{-1} (see Figure S8, Supporting Information). This synthetic procedure led to polymers which could be redissolved either in THF at room temperature (COOH molar incorporation ≥12 mol %) or in tetrachloroethane at 120 °C (COOH molar incorporation <12%). However, it should be noted that complete dehydration (for example by heating a polymer above its melting point) resulted in a polymer, which in our hands was insoluble due to the formation of intermolecular H-bonds (as indicated by FTIR spectroscopy). Analysis of quantitative ^{1}H and ^{13}C NMR spectra recorded at room temperature for PEAAx samples of AA ≥ 12 mol % or at 120 °C for PEAAx samples of AA < 12 mol % (Figures S5 and S6, Supporting Information) confirmed that the copolymers were fully and cleanly deprotected. Thus, the ^{1}H NMR spectrum resonance at 1.95 ppm due to the methine protons C*H*(COO^{t}Bu) was replaced by a signal at 2.2 ppm attributed to the methine protons C*H*(COOH). In the case of copolymers containing 12 mol % AA and more, the molar incorporation of COOH was measured also by conductometric titrations (see Figure S9, Supporting Information) that yielded values in excellent agreement with data derived from quantitative NMR spectroscopy (Table 1).

Bulk Properties of Copolymers. Differential scanning calorimetry (DSC) measurements were carried out on copolymer samples heated at a rate of 0.3 °C/min following a pretreatment from 140 to 20 °C at a cooling rate of 0.3 °C (Figure 1, Table 1). The DSC traces of PETBAx samples present a single endothermic peak, from which we extracted the enthalpy of melting (ΔH) and the melting temperature (T_m). The ΔH values decreased significantly with increasing TBA incorporation; for example, the ΔH of PETBA16 is more than 10 times smaller than that of PETBA4, and 20 times smaller than that of pure polyethylene prepared under the same conditions, indicating that PETBA16 is nearly totally amorphous. This is confirmed by the X-ray powder diffraction (XRD) pattern of this sample (Table 2) for which an amorphous broad peak dominates all other reflections. It is customary to calculate crystallinity by normalizing the enthalpy of melting of a copolymer by the enthalpy of melting of 100% crystalline polyethylene (294 J/g).[41] This calculation implicitly assumes that the crystallite is identical to that of pure polyethylene. We will see below that it is not the case with the samples described here, hence the PETBAx crystallinity values cannot be determined by this method.

(34) Piche, L.; Daigle, J.-C.; Poli, R.; Claverie, J. P. *Eur. J. Inorg. Chem.* **2010**, DOI: 10.1002/ejic.201000533.
(35) Guironnet, D.; Roesle, P.; Ruenzi, T.; Gottker-Schnetmann, I.; Mecking, S. *J. Am. Chem. Soc.* **2009**, *131*, 422–423.
(36) Ma, Q.; Wooley, K. L. *J. Pol. Sci., A: Polym. Chem.* **2000**, *38*, 4805–4820.
(37) Otocka, E. P.; Kwei, T. K. *Macromolecules* **1968**, *1*, 244–249.
(38) Jung, M. E.; Lyster, M. A. *J. Am. Chem. Soc.* **1977**, *99*, 968–969.
(39) Olah, G. A.; Liang, G.; Schleyer, P. v. R.; Parker, W.; Watt, C. I. F. *J. Am. Chem. Soc.* **1977**, *99*, 968–969.
(40) Xiang, M.; Jiang, M.; Kong, X.; Yang, Y.; Lu, W. *Macromol. Rapid Commun.* **1997**, *18*, 385–391.
(41) Bandrup, J.; Immergut, E. H., Eds. *Polymer Handbook*; 3rd ed.; Wiley Interscience: New York, 1989.

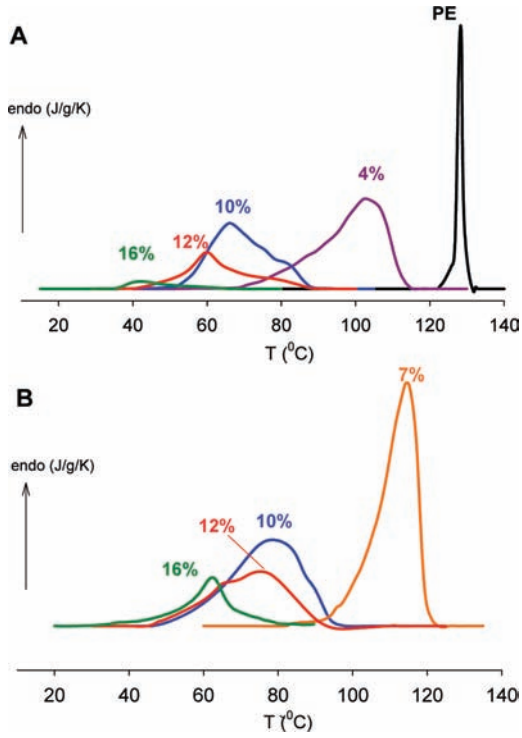

Figure 1. DSC melting endotherms of bulk PE, PETBA*x* (A), and PEAA*x* (B); the % values represent the level of comonomer (TBA or AA) incorporation in mol %.

Table 2. X-ray Diffraction Data for Samples of PE and PEAAx[a]

polymer	angle 2θ (deg)	Debye−Scherrer particle size, nm	lattice spacing, Å
PE[b]	21.6[b]	nd	$b = 4.93$[b]
PE[b]	24.0[b]	nd	$a = 7.40$[b]
PEAA4	21.4	24	$b = 4.98$
PEAA4	23.8	24	$a = 7.46$
PEAA7	21.4	22	$b = 4.98$
PEAA7	23.7	22	$a = 7.50$
PEAA10	21.35	17	$b = 4.97$
PEAA10	23.5	17	$a = 7.58$
PEAA12	21.25	15	$b = 4.99$
PEAA12	23.3	15	$a = 7.62$
PEAA14	21.2		
PEAA16	amorphous		
PEAA17	amorphous		

[a] For copolymers with AA incorporations larger than 14 mol %, the amorphous broad peak dominates and no separate reflection can be observed. [b] Data from reference 42.

The melting points (T_m) of the copolymers, also, decreased with increasing comonomer incorporation, and all values were lower than the T_m of PE, as shown in Figure 2, where we present a plot of the changes in T_m of PETBA*x* as a function of comonomer content. We included on the plot the T_m values of copolymers of ethylene and other nonionic monomers, such as poly(ethylene-co-methylacrylate) and poly(ethylene-co-*N*-vinylpyrrolidinone), which were prepared by catalytic copolymerization using the same catalyst (**1**, Scheme 1) as in the synthesis of the PETBA*x* samples.[30,32] The melting points of all the copolymers fall on the same line, in agreement with the Flory exclusion model,[42] which stipulates that the substituents introduced by a comonomer are excluded from the PE crystallite.

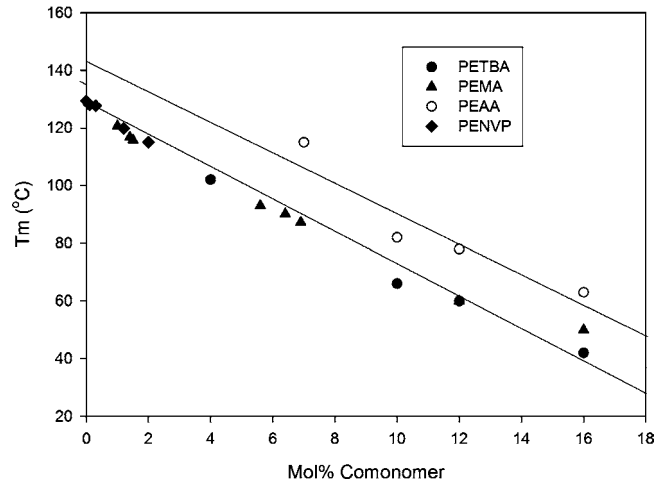

Figure 2. Changes of the melting point (T_m) of copolymers prepared by catalytic polymerization as a function of comonomer incorporation (in mol %). The melting points of PEMA (poly(ethylene-co-methyl acrylate) and PENVP, poly(ethylene-co-*N*-vinylpyrrolidinone), are taken from ref 32. The lines are to guide the eye.

Increasing comonomer incorporation results in smaller crystallites and lower melting points, irrespective of the nature of the comonomer. The melting points of the PEAA*x* samples are also shown in Figure 2. They are systematically higher by ~10 °C, compared to their PETBA*x* precursors and deviate significantly from the Flory exclusion model line constructed using melting points of copolymers of ethylene and nonionic polar monomers (Figure 2). This observation necessarily implies that some of the COOH groups may in fact be included in the PE crystal cell. Further support for this hypothesis was gathered by analysis of XRD data recorded for bulk copolymers. The diffraction pattern of each copolymer was resolved into two peaks, one at an angle $2\theta = 21.3 \pm 0.2°$, corresponding to the 110 reflection, and the other one at $2\theta = 23.5 \pm 0.2°$, corresponding to the 200 reflection, both for an orthorhombic unit cell (see Figure S10, Supporting Information). These reflections were used to calculate the dimensions of the copolymers unit cell that are listed in Table 2, together with the known dimensions of the unit cell of orthorhombic polyethylene ($a = 7.40$ Å and $b = 4.93$ Å).[42] For all copolymers, the *a* spacing is significantly larger than the *a* value of the polyethylene unit cell, while the *b* spacing is identical, or very close, to the *b* spacing of pure polyethylene (Table 2). This lattice expansion must be ascribed to the accommodation of some, but not necessarily all, COOH groups as crystalline defects in the PE crystals. This observation is in good agreement with existing data for 'precision' PEAA samples prepared by ADMET.[17,43] These defects are generally expected to weaken the crystal cell (lower melting point), but in our case, intracrystalline H-bonds due to adjacent COOH groups can reinforce the crystals and enhance their melting point.

Amphiphilic Properties of Poly(ethylene-co-AA) and Nanoparticle Formation. Among the various copolymers prepared, only PEAA12 is both crystalline and readily soluble in organic solvent. Samples of lower AA content are crystalline but only scarcely soluble at ambient temperature, while samples of higher AA content dissolve readily in organic solvents but are not crystalline. Since one specific objective of this study was to

(42) Takahashi, Y.; Ishida, T. *J. Polym. Sci., Polym. Phys.* **1988**, *26*, 2267–2277.

(43) Lehman, S. E.; Wagener, K. B.; Baugh, L. S.; Rucker, S. P.; Schulz, D. N.; Varma-Nair, M.; Berluche, E. *Macromolecules* **2007**, *40*, 2643–2656.

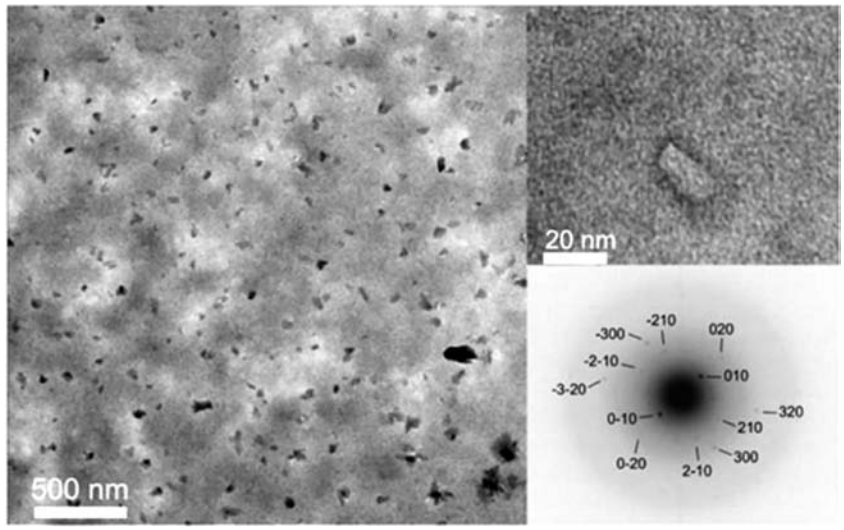

Figure 3. TEM micrographs of nanoparticles obtained from dialyzed suspensions of PEAA12 (upper right: enlarged view of one of the particles; lower right: electron diffraction pattern obtained for one nanoparticle).

assess the impact of crystallinity on the self-assembly of amphiphilic copolymers in water, we focused our attention to the properties of PEAA12 in solution in THF containing aqueous sodium hydroxide (0.02 N). The resulting mixture was subjected to extensive dialysis against water to remove excess NaOH and THF. This procedure led to the formation of an opalescent fluid (pH = 7). The size and size distribution of the nanoparticles in suspension were determined by dynamic light scattering (DLS) measurements carried out with a fluid for which the copolymer concentration was adjusted to 1.0 g L^{-1}. The major population of objects in this fluid has an average hydrodynamic radius (R_h) around 12 nm. A minor population, representing less than 5% in weight, was detected in the larger size domain ($R_h \sim 88$ nm). Visualization by TEM of the air-dried fluid confirmed the presence of nanoparticles. The micrographs feature elongated objects, with an average polar radius of 49 nm ($\sigma = 15.0$ nm) and an equatorial radius of 9 nm ($\sigma = 3.0$ nm), together with a few occasional larger particles (Figure 3, and Figure S11, Supporting Information). The discrepancy between the nanoparticles radii measured by DLS and TEM is to be expected when one recalls that the hydrodynamic radius of nonspherical particles is not equal to their geometrical radii. The hydrodynamic radius obtained from DLS measurements derives, via the Stokes−Einstein equation, from the nanoparticle self-diffusion coefficient, which for an elongated particle of length L and cross-section d in water of viscosity η at a temperature T, can be expressed as

$$D = \left(\frac{k_B T}{3\pi\eta L}\right)\left(\ln p + 0.312 + \frac{0.565}{p} - \frac{0.100}{p^2}\right) \qquad (1)$$

where $p = L/d$.[44,45] Using the values of L and d obtained by TEM, the calculated value of D is 2.09×10^{-11} m^2 s^{-1} at 25 °C. The Stokes−Einstein formula ($D = k_B T/6\pi\eta R_h$) can then be used to calculate a hydrodynamic radius R_h of 11.7 nm, a value which is in excellent agreement with the DLS measurement.

The morphology of the rod-like particles is reminiscent of the shape of the surfactant-stabilized nanoplatelets of pure crystalline PE obtained by catalytic emulsion polymerization of ethylene in water.[25] It suggests that the colloidal PEAA12 nanoparticles contain crystalline domains. Analysis of single nanoparticles by high-resolution transmission electron microscopy (HRTEM) yielded electron-diffraction patterns (Figure 3) consistent with the orthorhombic lattice of a PE monocrystal ($a = 7.37$ Å and $b = 4.93$ Å).[45] This demonstrates that each nanoparticle, which was colloidally stable in water, contains in fact one isolated monocrystal. However, the point to point resolution of the pattern is not sufficient to ascertain whether the monocrystal lattice is that of pure PE or that of a slightly dilated PE cell in which COOH groups are present.

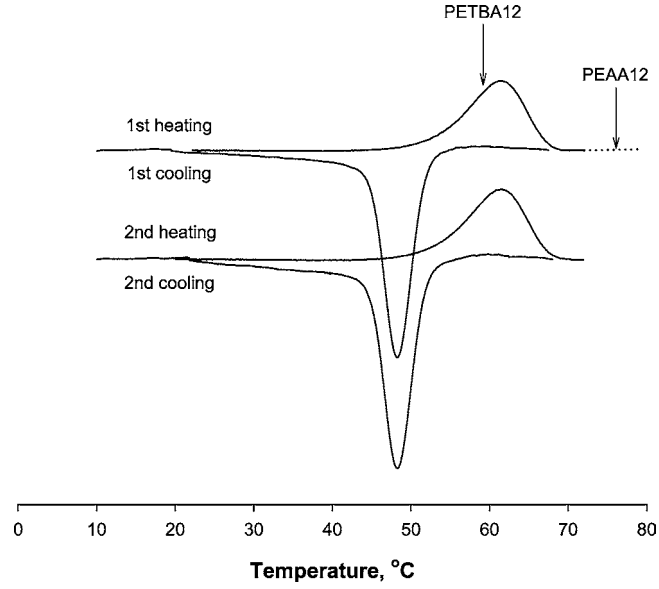

Figure 4. Thermograms of an aqueous dispersion of PEAA12 in water (~1 g/L) recorded by HS-DSC upon heating and subsequent cooling (heating/cooling rate: 1 °C/min). The arrows indicate the melting points of solid PETBA12 and PEAA12.

Temperature-Responsiveness of Aqueous Colloidal Poly(ethylene-co-AA) Fluids. A high-sensitivity DSC scan recorded upon heating a colloidal suspension of PEAA12 ($c = 1.0$ g L^{-1}) at a rate of 1.0 °C per min is presented in Figure 4, together with the scan recorded upon cooling the sample at the same rate.

(44) Pecora, R. *J. Nanopart. Res.* **2000**, *2*, 123–131.
(45) Tirado, M. M.; Garcia de la Torre, J. *J. Chem. Phys.* **1979**, *71*, 2581–2587.
(46) Yin, L.; Chen, J.; Yang, X.; Zhou, E. *Polymer* **2003**, *44*, 6489–6493.

The trace corresponding to sample heating presents an endotherm with a maximum (T_m^{coll}) at 62 °C and an enthalpy of 81 J/g. Upon cooling, an exotherm is observed at a temperature of 48 °C, which is 14 °C lower than the transition taking place upon heating. Rescanning the sample under identical conditions gave identical thermograms. Turning our attention first to the heating scan, we note that the T_m^{coll} is nearly identical to the melting temperature of bulk PETBA12 bulk (60 °C, see Figure 1 and Table 2). This similarity suggests that the endothermal transition observed when heating the nanoparticles in water corresponds in fact to the melting of the crystals within the nanoparticles. This hypothesis is strengthened by two additional facts: (i) the difference between temperature maxima recorded upon heating and subsequent cooling is reminiscent of the supercooling effect expected for a polymer crystallization process. A supercooling effect of 70 °C has been reported recently for the melting/crystallization of polyethylene nanoparticles;[25,47] (ii) the T_m^{coll} value is different from the T_m of bulk PEAA12 (76 °C, see Figure 1A and Table 2) but corresponds to the melting point of bulk PETBA (see above). This observation implies that the endotherm observed reflects the melting of crystalline PE, as in the case of PETBA12 (see above), rather than the melting of a crystal that incorporates COOH defects within its lattice, as in the case of bulk PEAA12. The enthalpy of the transition of the aqueous colloidal PEAA12 dispersion does not correspond to the enthalpy of bulk PETBA12. It is significantly larger (81 J/g vs ~44 J/g for PEAA12 and 18 J/g for PETBA12 from Figure 2). Thus, the melting of the PE crystalline phase of suspended nanoparticles must be accompanied by additional endothermal effects, which accompany changes in the interactions of the nanoparticles with their aqueous environment. From the HS-DSC results and the electron diffraction patterns, which prove that the nanoparticles contain a single monocrystal and an amorphous phase, we speculate that in the aqueous environment the energy gained during crystallization ($-\Delta H_{melting}$) is not sufficient to offset the heat of solvation of the partially deprotonated COOH (at pH = 7, with Na^+ or H^+ counterions), forcing most polar substituents to stay in the amorphous phase when the crystal is formed. Furthermore, the presence of hydrophilic groups on the particle surface accounts for the colloidal stability of aqueous PEAA12 suspensions.

To probe the fate of the nanoparticles upon heating, we performed DLS measurements on aqueous colloidal PEAA12 suspensions heated to several temperatures between 20 and 65 °C. Representative size distributions are presented in Figure 5. At 20 °C, the suspension contains mainly particles of $R_h = 12$ nm as noted above. No significant changes are observed upon heating up to 55 °C. Above this temperature, the scattering profile has a significant contribution from particles of $R_h \sim 240$ nm, which become the major contributors in suspensions heated to 65 °C, i.e., above the melting temperature of PE. Hence, the originally crystalline nanoparticles coalesce into larger "nanodroplets", which remain colloidally stable in hot water and do not undergo macroscopic phase separation. The term "droplet" is an apt description of the particles, since the PE is in its liquid state at this temperature. Assuming that a droplet has approximately the same density as an elementary nanoparticle, we estimate that a droplet is composed of about 180 elementary nanoparticles. The coalescence of nanoparticles is believed to be triggered by the conservation of the interfacial energy upon melting of the PE crystal and reorganization of the interfacial structure associated with the enthalpy detected by HS-DSC measurements.

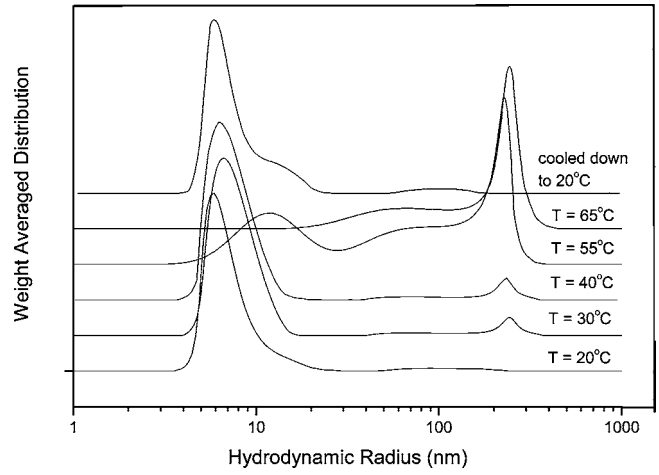

Figure 5. Hydrodynamic radii distributions recorded by DLS for a suspension of PEAA12 in water heated to various temperatures from 20 to 65 °C. The top trace corresponds to a sample cooled from 65 to 25 °C.

The topmost size distribution presented in Figure 5 corresponds to a sample cooled from 65 to 25 °C and kept at this temperature for several hours. Remarkably, it is identical to the size distribution of the suspension prior to heating. The heating/cooling cycle was repeated three times without any changes in particle size distributions of either the cold or hot suspensions. Thus, upon reaching the PE crystallization temperature, the droplet crystallizes and fragments to form crystalline nanoparticles of dimensions identical to those of the original particles.

Conclusions

This work demonstrates that the most common polyolefin, namely polyethylene, can form well-defined surfactant-free nanoparticles that are colloidally stable in water. In order for polyethylene to be dispersible in water, pendant COOH groups were introduced along the linear chain. The resulting polymer, linear PEAA, crystallizes in the bulk in the usual orthorhombic polyethylene unit cell, where one of the cell dimensions is elongated in order to accommodate COOH groups as defects in the crystal.[42] The presence of H-bonded COOH groups within the crystal results in an increase of the melting point of the copolymer, in comparison to the melting point predicted by the Flory exclusion model. Using a solvent exchange procedure, followed by a dialysis, we were able to trigger the self-assembly of a PEAA copolymer with 12 mol % AA into nanoparticles freely suspended in water. Using a combination of electron diffraction and HS-DSC studies, we established that these particles are in fact composed of a core of pure polyethylene surrounded by a hydrated layer containing the COOH groups. Thus, the nanoparticles and the bulk polymer can be seen as two allomorphic forms of the same polymer. The crystallization into one or the other allotrope is directed by the presence (or absence) of water. Although well documented for small molecules, this behavior is rather uncommon for macromolecules. Heating a suspension past the nanoparticle melting temperature triggers the coalescence of melted nanoparticles into nanodroplets of finite dimensions. This behavior is reversible: cooling the suspension below the copolymer melting point triggers the formation of colloidally stable crystalline nanoparticles similar in size to the nanoparticles prior to the heating/cooling treatment. Hence, the polyethylene nanoparticles are thermoresponsive. This

(47) Bauers, F. M.; Thomann, R.; Mecking, S. *J. Am. Chem. Soc.* **2003**, *125*, 8838–8840.

intriguing and novel thermoresponsive behavior of ethylene copolymers opens the way to interesting applications as, for example, for the generation of stimuli-responsive nanomaterials for biomedical or environmental uses.

Acknowledgment. Financial support for this work was provided by the Fonds Québécois de la Recherche sur la Nature et les Technologies. F.M.W. thanks Prof. T. Sato (Osaka University, Toyonaka, Osaka, Japan) for useful comments and suggestions on the work.

Supporting Information Available: Experimental procedures as well as characterization (^{1}H NMR and ^{13}C NMR spectra of PETBA*x* and PEAAx, GPC traces, X-ray powder diffraction patterns, FTIR spectra of PETBA*x* and PEAAx, conductometric titration curves, additional DLS data). This material is available free of charge via the Internet at http://pubs.acs.org

JA104182W